XL CILAMCE
IBERO-LATIN AMERICAN CONGRESS ON COMPUTATIONAL METHODS IN ENGINEERING
NOVEMBER 11-14, 2019
Praiamar Natal Hotel & Convention
Natal, RN-BRAZIL

SENSITIVITY ANALYSIS BASED ON MORRIS SCREENING METHOD FOR BLADE DESIGN OF A CENTRIFUGAL COMPRESSOR

Vitor Cesar N. Mattos
Elóy E. Gasparin
vitormattosn@gmail.com
eloygasparin@gmail.com
Dept. of Mechanical Engineering, Sao Paulo State University
Ilha Solteira, 15385-000, SP, Brazil
Paulo Eduardo B. Mello
Dept. of Mechanical Engineering, Educational Foundation of Ignatius Father Sabóia de Medeiros
São Bernardo do Campo, 09850-901, SP, Brazil
Fábio Saltara
Dept. of Mechanical Engineering, University of São Paulo
São Paulo, 05508-970, SP, Brazil
Daniel J. Dezan
Engineering, Modeling and Applied Social Sciences Center, Federal University of ABC
Santo André, 09210-580, SP, Brazil
Jurandir I. Yanagihara
Dept. of Mechanical Engineering, University of São Paulo
São Paulo, 05508-970, SP, Brazil
Leandro O. Salviano
leandro.salviano@unesp.br
Dept. of Mechanical Engineering, Sao Paulo State University
Ilha Solteira, 15385-000, SP, Brazil

Abstract. Sensitivity Analysis is an important tool for works that have a several number of input variables which can influence the final results when the goal is enhancement of any machine or system. For centrifugal compressors, the efficiency depends on the behavior of several phenomena such as shock waves and recirculation, which these effects are dependent of the geometry parameters as thickness, angle and shape. In order to find the influence of the thickness and distance between main blade and splitter on total isentropic efficiency, an Elementary Effects analysis associated to a robust CFD model using ANSYS CFX was performed, considering a 4:1 compressor known by NASA CC3. The results indicate that the thicknesses at medium spanwise position are more important than those at border. Furthermore, the leading-edge parameters are also more influent than those in trailing-edge. Finally, four variables are found as no significant effect and other five can be used for future analysis as optimizations reducing computational cost. The work also shows that the variation on efficiency is closely connected with the changes in most influent parameters due to its geometric changes in specifically regions which are immersed in the source of losses cited previously.

Keywords: Morris screening, Centrifugal compressor, Sensitivity analysis, Impeller CFD model.

1. Introduction

Centrifugal compressors are rotating machines present in several industry applications, such as refrigeration, air-conditioning, power generation and household appliances. This component can lead to complex turbulent flows with recirculation and adverse pressure gradient, making the design of a high-performance turbomachinery a great challenge for engineers. due to several parameters like blade thickness, blade meridional shape and blade angles that can impact its efficiency. In general, one-dimensional systems, such as Meanline method [1] and Streamline Curvature method [2] are strongly applied on industries, being useful as starting design point. However, the authors assert that these models cannot replace more modern three-dimensional methods. Therefore, for more accuracy and precision, Computational Fluid Dynamics (CFD) has been widely used in past twenty years due to CPU power increasing.

Marconcini et al. [4] and Ibaraki et al. [5] previously identified in them work phenomena that cause severe losses for continuity of flow. Both cited two main effects that appears in several centrifugal compressors: shock waves at inlet that create adverse gradient of pressure due to sudden increase pressure and caused by high velocities and recirculation throughout the passage volume. Thus, this work uses a methodology called Sensitivity Analysis associated with CFD for identify these main phenomena and the influence that the geometry has on them.

Sensitivity Analysis (SA) is a statistical tool that studies how the model input variables affects the interest outputs, describing the importance of each input in determining the outputs variability. There is a large number of SA methods available starting from qualitative screening methods to quantitative variance based methods [6]. The Elementary Effects (EE) Method introduced by Morris (1991), refined by Campolongo; Cariboni and Saltelli, (2007) is considered a good practice in SA for large and expensive computational models. This screening method seeks to identify the non-influential input variables using a small number of original model runs and has been effective [6].

Then, for all these analyses the NASA CC3 was the machine chosen because its experimental data is widely publicized and exist several articles aiming to study it [9], [10]. Furthermore, this turbomachine is a high performance 4:1 pressure ratio centrifugal compressor with aim to substitute its old version to improve the mass flux and the aerodynamic parameters [11].

This study aimed to perform the CFD validation of NASA CC3 compressor impeller and sensitivity analysis, explaining its results based in the phenomenological aspects of the tridimensional model, allowing to assess which inlet variables are most influent. In addition, it can provide a reliable fixing of variables that are non-influent, turning a possible CFD model optimization process much faster.

2. Methodology

2.1 Governing equations

The flow is assumed to be steady-state as suggests Benini et al. [3] because the fluctuations are important only in impeller-diffuser gap and this work will not deal with this region. Furthermore, it is considered as turbulent, three-dimensional and the fluid model as ideal gas and pure substance. Hence, for a Newtonian fluid, the mass conservation, momentum and energy equations shown respectively in Eq. (1), Eq. (2) and Eq. (3) are applied to a finite volume-based commercial software.

However, the flow needs one more approach because a pure steady-state flow with simple equations of mass conservation and momentum does not consider the turbomachine rotation losing terms like centrifugal forces, Coriolis acceleration and relative velocities. Therefore, it was necessary to apply a rotating frame quantities model that inserts the rotation term into the velocity equation. It makes the solution to create a relative velocity for the stationary domain which can be understood as relative velocity (w) of turbomachinery and represents the real flow through domain. The other

velocity called stationary frame of reference velocity can be understood as real velocity (c) where will it be calculated parameters like enthalpy and entropy that should consider the rotation for real results

$$\nabla \cdot (\rho U) = 0 \tag{1}$$

$$\nabla \cdot (\rho U \times U) = -\nabla p + \nabla \cdot \tau + S_M \tag{2}$$

$$\nabla \cdot (\rho U I) = \nabla \cdot (\lambda \nabla T) + \nabla \cdot (U \cdot \tau) + U \cdot S_M + S_E \tag{3}$$

where τ is the stress tensor and accordingly to the rotating frame of reference equations of ANSYS CFX®: $S_M = S_{M,rot} = S_{cor} + S_{cfg}$. In which $S_{cor} = -2\rho\,(\omega \times \boldsymbol{U})$ (Coriolis Force) and $S_{cfg} = -\rho\,\omega \times (\omega \times \boldsymbol{r})$ (Centrifugal Force) and the rothalpy is $\boldsymbol{I} = h_{stat} + 1/2\,U^{\mathbf{2}} - \omega^{\mathbf{2}} R^{\mathbf{2}}$.

The turbulence method used is k-ω Shear-Stress Transport which considers different treatments between boundary layer – k-ω – and free shear flow – k-ε from two eddy-viscosity equations shown in Eq. (4) and Eq. (5)[12]. These characteristics make this model more robust and accurate when high adverse pressure gradients [12] as those present in centrifugal compressors are verified [13].

$$\frac{\partial(\rho U_j k)}{\partial x_j} = \frac{\partial}{\partial x_j}\left[\left(\mu + \mu_T \sigma_k\right)\left(\frac{\partial k}{\partial x_j}\right)\right] + P_k - \beta' \rho k \omega \tag{4}$$

$$\frac{\partial(\rho U_j \omega)}{\partial x_j} = \frac{\partial}{\partial x_j}\left[\left(\mu + \mu_T \sigma_\omega\right)\left(\frac{\partial \omega}{\partial x_j}\right)\right] + \alpha \frac{\omega}{k} P_k - \beta \rho \omega^2 + P_{\omega b} \tag{5}$$

Where the production term has been modified accordingly to Spalart [14], to better fit the streamline curvature and rotational system. To ensure robustness, an automatic near wall treatment as shown in Eq. (6), (7) and (8) is applied in regions where the value of y^+ is greater than one. The ω_l term represents this treatment in logarithmic region (turbulent layer) and the ω_s represents the viscous sublayer while ω_w is a smooth blending between two regions in order to achieve a formulation for the buffer layer.

$$\omega_l = \frac{u^{*2}}{a_1 \cdot k \cdot \nu \cdot y^+} \tag{6}$$

$$\omega_S = \frac{6\nu}{\beta(\Delta y)^2} \tag{7}$$

$$\omega_w = \omega_S \sqrt{1 + \left(\frac{\omega_l}{\omega_S}\right)^2} \tag{8}$$

Menter and Knopp [15], [16] append that these equations help the turbulence model to find accurate results even with the condition of low near wall distance not being fulfilled. Their approach suggests the results are reliable for values of y^+ up to ten as can be seen in Fig. 1 when it is compared to different treatments and even the analytical expression.

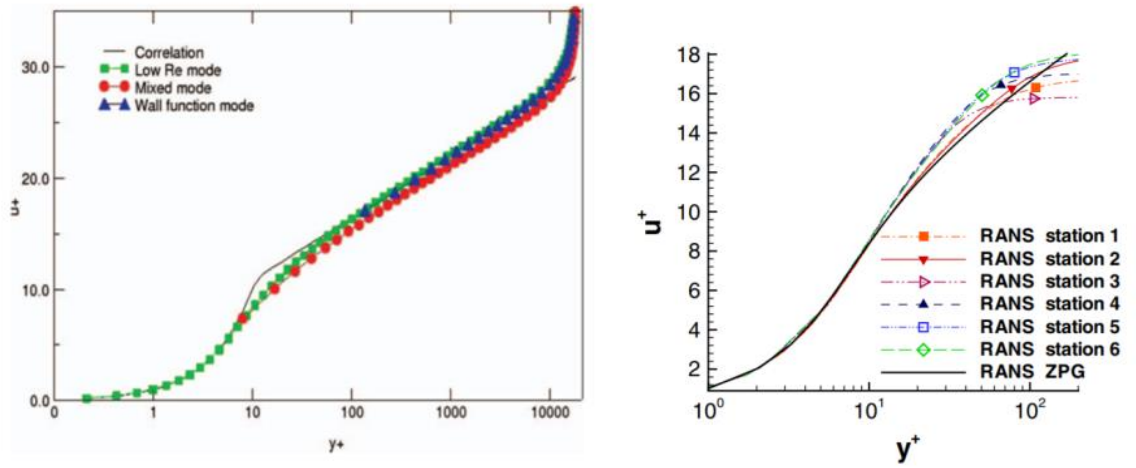

Figure 1. Automatic wall treatment [15], [16]

2.2 Computational domain and boundary conditions

The geometric data presented in Tab. 1 are characterized as a function of normalized streamwise ($M\%$), geometric blade angle (θ), normal thickness of the blade (T) and its meridional dimension (R is radial distance and Z is axial distance) as shown in Fig. 2 [11]. In addition, it can be noted the reference point (0,0) and the projection of the blade in meridional plane (ZR).

Table 1. Geometric data of NASA CC3

M%	R_{Hub} (mm)	Z_{Hub} (mm)	R_{Shroud} (mm)	Z_{Shroud} (mm)	T_{Hub} (mm)	T_{Shroud} (mm)	θ_{Hub} (º)	θ_{Shroud} (º)
0	41.44	0	104.96	0	3.37	1.92	1.6	0
20	56.52	46.05	108.57	36.34	6.71	3.17	28.8	22.8
40	82.56	86.91	121.85	70.20	7.41	2.90	39.4	36.7
60	120.81	116.39	145.23	98.28	7.84	2.67	45.5	45.4
80	167.22	129.64	178.62	112.65	8.73	2.66	53.2	52.7
100	215.75	132.24	215.72	115.20	11.76	2.92	65.2	62.0

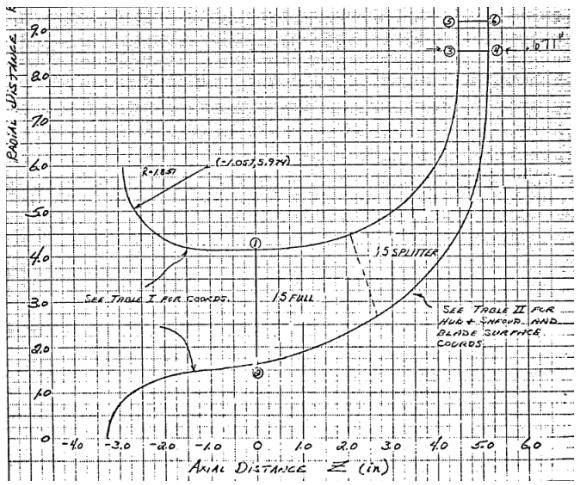

Figure 2. Meridional shape of blade [11]

It should be clarified that only the analysis of the impeller without diffuser ("vaneless diffuser

analysis") was performed initially, given that the beneficial effects of impeller-diffuser interaction on overall stage performance come mainly from the reduced blockage and reduced slip in the impeller, not from the diffuser itself [17].

Thus, it was created a computational model of the fluid passage through entire impeller based on previously cited geometry shown in left side of Fig. 3. But due to the periodic characteristics and geometrical symmetry, only one periodical part of the compressor impeller was computed as shown in right side of Fig. 3 and the results are extrapolated to remainder of the impeller decreasing the number of elements on the grid and computational cost. So, the basic domain is treated as static but rotational terms like centrifugal velocity, centrifugal forces and Coriolis acceleration are inserted in governing equations as shown previously turning it into a periodic rotational domain called stationary frame (Stn) [18] and all the properties are calculated by this frame. This method is inserted on ANSYS CFX solver, used in this study.

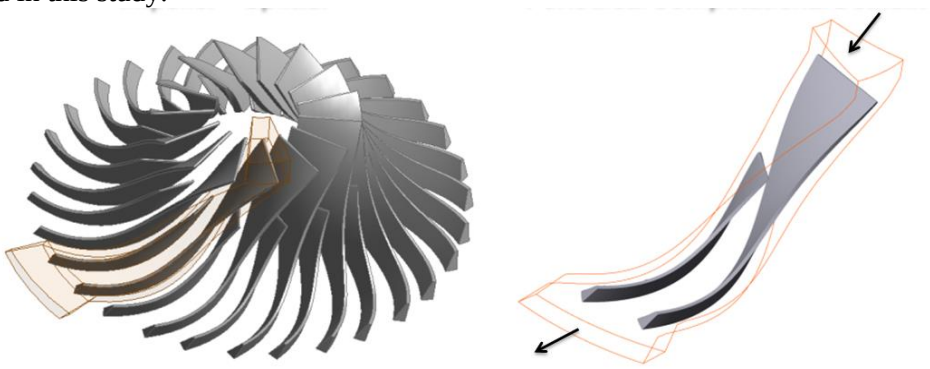

Figure 3. Three-dimensional shape of impeller (left) and the computational domain (right)

Finally, the fluid which pass in this domain is ideal air, entering in ambient conditions with small turbulence at inlet and at a mass flow of 4,536 kg/s (10lb/sec). Also, the walls are considered smooth and adiabatic with no slip [9], [10]. Tab 2 shows the main boundary conditions applied to setting the pre-processing.

Table 2. Boundary conditions for NASA CC3 [9], [10]

Rotation velocity	21789 rpm
Mass flux	4,536 kg/s
Inlet pressure	101283,98 Pa
Inlet temperature	288,17 K
Inlet turbulence	1%
Clearance gap	0,61 mm
Wall condition	No slip
Roughness	Smooth Wall

2.3 Mesh and quality criteria

One of the most important phases is the computational domain discretization because it may impair convergence and even accuracy. Therefore, a commercial software called ANSYS TurboGrid was chosen for this task since it's successfully cited in several articles [10], [19] in this field due to its robustness and ease to use for turbomachinery.

To prevent that the generated mesh implies in these situations for solution, four criteria were analyzed as CFX Theory Guide suggests [18]: orthogonal angle, expansion factor, aspect ratio and y^+ which represents a function of near-wall distance and flow dynamic. The first two quality parameters

presented were within the acceptable range while the other two had some elements that were out did not jeopardized simulation convergence as will be seen further.

Several grids were tested and the one with best results in accuracy and processing time was chosen. The entire domain, near-wall refinements and the shape of elements used can be seen in Fig. 4.

Figure 4. Entire meshed domain

The low value of y^+ and high values of velocity and rotation explain the high value of aspect ratio shown in Tab. 3. It is necessary an element with small length in the normal direction of walls but the same doesn't occur in other direction increasing the dimension relation. To reach acceptable levels of aspect ratio, a refinement was applied and it was encountered a grid with few "bad" elements (about 0.002% of all elements) as shown in red in Fig. 5 which promoted good convergence and accuracy.

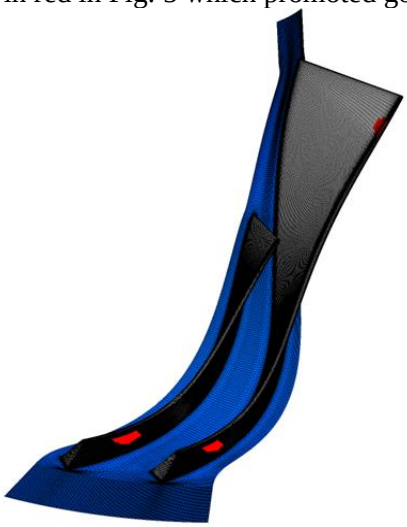

Figure 5. Regions with high aspect ratio

The same grid provides a y^+ greater than one getting out of what is suggested by used turbulence model SST k-ω [12] but the right side of Fig. 6 and Tab. 3 show that values greater than five are found just in a few regions and the maximum value is about eleven so it is possible to conclude that the grid is within acceptable range for near-wall automatic treatments applied in CFX [15], [16], [18] and seen in this work previously.

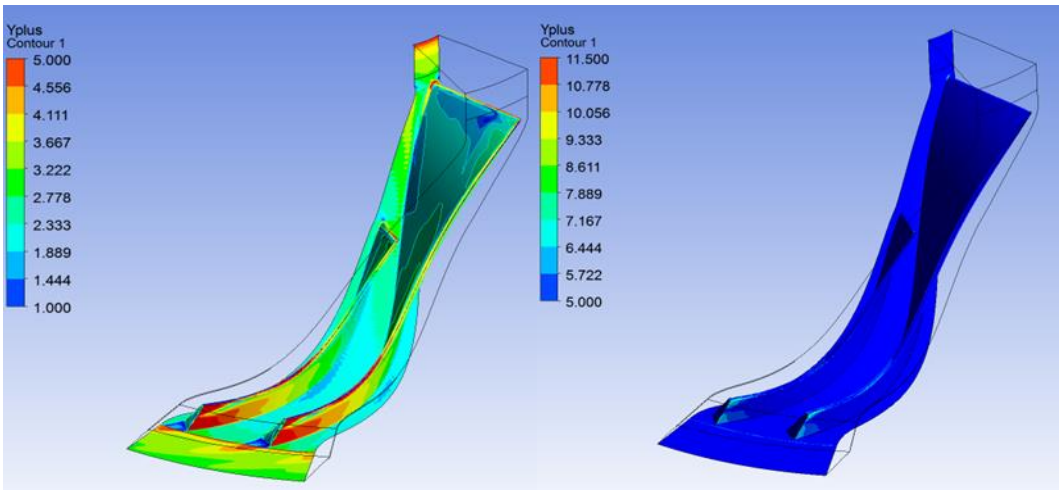

Figure 6. Turbulence criteria

Table 3. Mesh criteria

Maximum aspect ratio	Maximum expansion factor	Minimum orthogonal angle	y+ max	y+ med	y+>5
1716	15,9	31,9º	11.42	2.86	86%

2.4 Grid Independence and numerical validation

The mesh validity is based on Grid Convergence Index Method (GCI), an acceptable and a recommended method that compare three meshes with different refinement. If authors choose to use it, the method per se will not be challenged in the paper review process [20]. Therefore, the three grids based on this approach are created and its parameters as its graphic representation are shown in Tab. 4 and Fig 7 respectively.

Table 4. GCI parameters

	Grid 1	Grid 2	Grid 3
Cells number, n	1.402×10^{6}	3.868×10^{6}	10.805×10^{6}
Mesh size, $h = (V/n)^{1/3}$	6.61×10^{-3}	4.72×10^{-3}	3.35×10^{-3}
Refinement factor, r	-	1.41	1.40

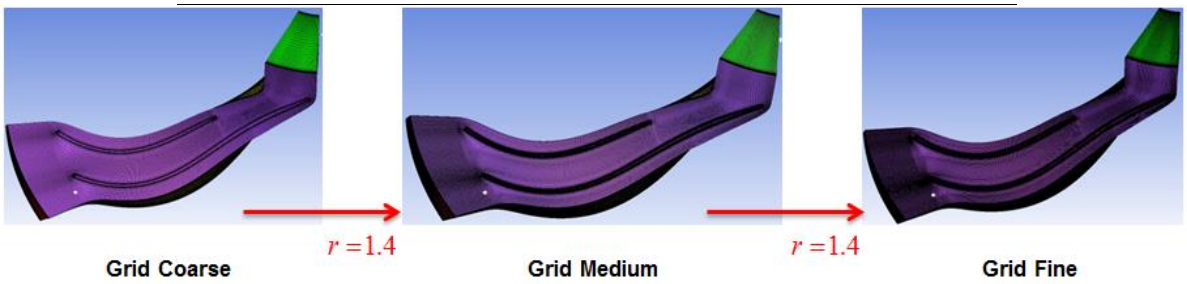

Figure 7. Three GCI grids

Notice that the grid refinement factor r is greater than 1.3 as recommended by Celik et al [20]. Thus, the procedure to determine the GCI for Total to Total Isentropic Efficiency, Pressure Ratio and Temperature Ratio was applied and the results are presented in Tab. 5. It can be concluded that the higher uncertainty is smaller than one percent for all factors. Therefore, the grid independence is checked and the medium grid may be used as a reference for other configurations of this research.

Table 5. GCI results

	Isentropic Efficiency	Pressure Ratio	Temperature Ratio
GCI	0.65%	0.003	0.05

After choosing the mesh which will be used for simulation, it was created another grid called "Refined Grid" whit maximum y^+ less than five to suit the turbulence model. Comparing with the results from the grid chosen by GCI it can be affirmed, from Tab. 6, that the medium grid is sufficient to this work since both solutions provide small differences from measured data lower [9].

Table 6. Numerical validation

Configuration	Isentropic Efficiency (%)	%	Pressure Ratio	%	Temperature Ratio	%
Measured Data	86.7	-	4.18	-	1.58	-
Grid chosen by GCI	86.49	0.24	4.156	0.62	1.596	1.01
Refined Grid	86.7	0.00	4.154	0.62	1.596	1.01

Thus, the medium grind using Automatic Wall Treatment in SST k-ω was chosen because it presented great computational benefits for sensitivity analysis and future optimizations without loss in the accuracy.

2.5 Geometrical parameters

The geometry generation of the impeller was done in ANSYS Blade Editor, which is a free hand tool to facilitate the generation of different blade models for turbomachinery. The software generates a geometry by parameters like blade meridional angle, thickness, meridional shape and flow path. Note in Fig. 8 that the purple and green lines represent the leading edge and the trailing edge of the blade, respectively while the other lines represent the fluid passage domain.

To proceed with sensitivity analysis, it's necessary to implement variables called parameters which allow automatic changes of values. As an initial study, to avoid expensive computational cost, the parameterization is focused only on blade thickness and distance between blade and splitter leaving aside meridional angle and meridional shape.

The thickness is set up as a function of streamwise and spanwise and need these cartesian points to specify the local control. Therefore, four layers are created to reference the variable in span direction as shown in left side of Fig. 9 allowing to change the thickness along the height of blade.

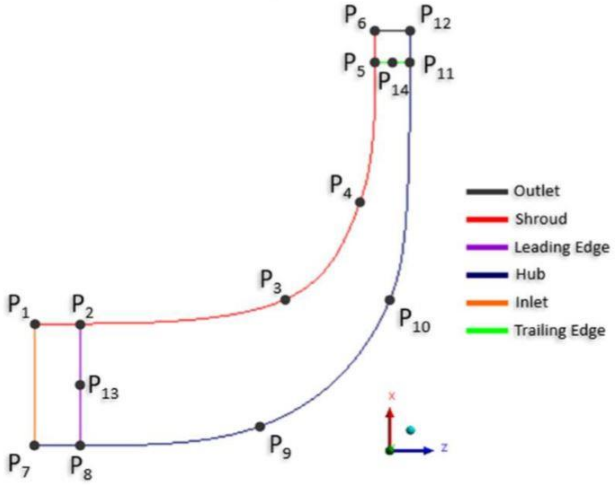

Figure 8. Meridional view of fluid-flow domain

To reference in stream direction, two control points with freedom in y-axis (normal layer thickness) and fixed in x-axis (streamwise) are created as shown in right side of Fig. 9 allowing to

change the thickness along the camber line.

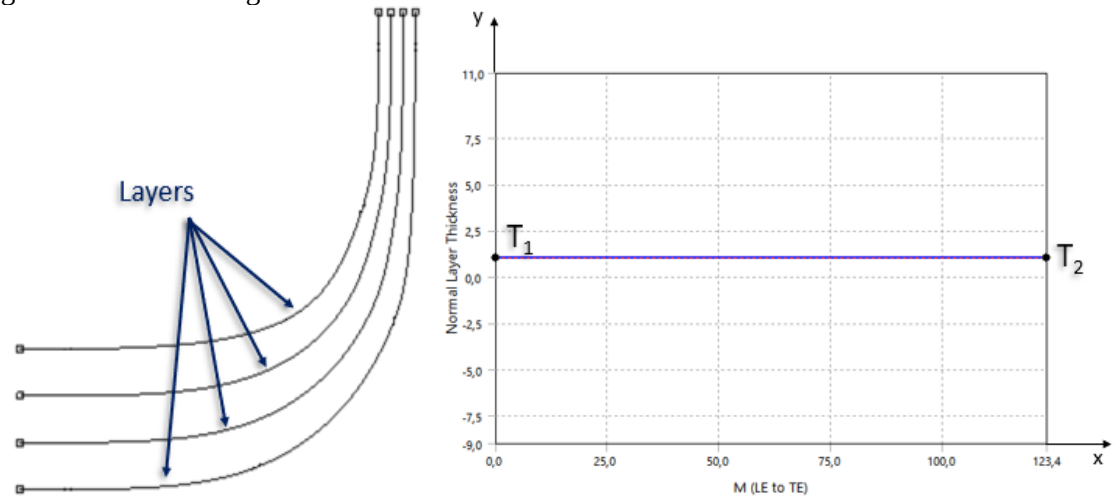

Figure 9. Thickness parameterization

The distance between blade and splitter (DESL) is set up as a function only of the meridional distance in fluid-flow domain. Thus, it's necessary specify only the meridional percentage distance desirable between two main blades in ANSYS Blade Editor.

Finally, the parameterization has an amount of nine variables which will be used and changed during the sensitivity analysis procedure.

3. Sensitivity Analysis

Associated with CFD, sensitivity analysis and optimization of engineering projects has become an increasingly popular tool. This analysis evaluates the change in the output parameters by changing the input parameters [21]. Bilal [22] states that the output parameters in the design of a centrifugal compressor vary significantly depending on geometric and operational parameters. In this way, several methods and techniques of sensitivity analysis have emerged as an alternative to allow the reduction of the amount of input parameters reliably and robustly, allowing a later optimization process to be faster and more assertive.

3.1 The elementary effects method

Morris [7] developed a sensitivity analysis method for computational models with moderate to large number of input parameters. The proposal was to perform a one-factor-at-a-time sensitivity analysis, choosing the input parameters randomly and determining which of them would have important effects on the output parameters, reducing 'sparsity' problems present in the screening. This method is known as the Elementary Effects (EE) Method, and recognized as a simple but effective way of screening a few input factors among the many that can be contained in a model. If a model has k independent inputs Xi, $(i = 1,..,k)$, for a given value of X, the Elementary Effect is defined by Eq.(9).

$$EE_i = \frac{Y(X_1, X_2, ..., X_i + \Delta, ..., X_k) - Y(X_1, X_2, ..., X_k)}{\Delta} \tag{9}$$

where Δ is the step in the discretized input space.

Morris [7], suggests sampling r elementary effects for each input variable via an efficient design that constructs r trajectories of $(k + 1)$ points in the input space. The total cost of the experiment is thus the number of trajectories multiplicated by number of independent inputs plus one.

The goal of the Morris original EE method is to determine which input factors may be considered

negligible, linear and additive or non-linear and involved in interactions with other factors. For each input, two sensitivity measures were proposed - μ, the average of each input EE distribution, which assesses the overall influence of the variable, and σ, the deviation of each input EE distribution, which estimates the influence in interactions with other factors. That two parameters are calculated from Eq. (10) and Eq. (11), respectively.

$$\mu_i = \frac{1}{r}\sum_{j=1}^{r} EE_i^j \tag{10}$$

$$\sigma_i = \frac{1}{r-1}\sum_{j=1}^{r} (EE_i^j - \mu_i)^2 \tag{11}$$

Campolongo, Cariboni and Saltelli [8], proposed a revised version of the measure μ, called μ^*, which on its own is sufficient to provide a reliable ranking of variables. The parameter μ^*, calculated from Eq. (12), is the average of the EE distribution in absolute values, solving the problem of effects having opposite signs which occurs when the model is non-monotonic.

$$\mu_i^* = \frac{1}{r}\sum_{j=1}^{r} \left| EE_i^j \right| \tag{12}$$

The use of μ^* convenient as it solves the problem of failing to identify a factor with considerable influence on the model, that can occur due to positive and negative effects canceling each other out when computing μ [23].

Campolongo, Cariboni and Saltelli [8] also proposed an improvement of the sampling strategy, which aims at a better scanning of the input domain without increasing the number of model executions needed. The r trajectories were selected in such a way as to maximize their dispersion in the input space. It starts generating a high number of Morris original trajectories ($M = 500 - 1000$), and then it chooses, r trajectories with the highest 'spread', based on the following definition of 'distance'. The distance d_{ml} between a couple of trajectories m and l is calculated according to Eq. (13).

$$d_{ml} = \begin{cases} \sum_{i=1}^{k+1}\sum_{j=1}^{k+1}\sqrt{\sum_{z=1}^{k+1}\left[X_i^m(z) - X_j^l(z)\right]^2}, & m \neq l \\ 0, & otherwise \end{cases} \tag{13}$$

where k is the number of input factors and $X_i^m(z)$ indicates the z^{th} coordinate of the i^{th} point of the m^{th} Morris trajectory.

Then, it considers for each possible combination of r trajectories the quantity D, which is the sum of all the distances between couples of trajectories belonging to the combination. Thus, it selects the combination with the highest value of D.

This sampling methodology is called optimal sampling as it checks all possible combinations of trajectories. However, as the total number of combinations considered at the optimal approach is $M!/[r!\,(M-r)!]$, for high dimensional and large models, the combinatorial optimization problem may turn the sampling process unfeasible for current computers. To overcome this problem Ge; Ciuffo and Menendez [24] proposes that instead of picking r optimal trajectories (OT) directly from the original set of M, the set of $(M-1)$ trajectories with the highest total distance is first picked; in the second step, the set of $(M-2)$ trajectories with the maximum dispersion is chosen. Such process is repeated until a set with only r trajectories is left. These r trajectories are called the quasi-Optimized Trajectories (quasi-OT). The total number of combinations considered in this approach is $(M + n)(M - n + 1)/2$. The validation tests indicates that the quasi-OT are very close to the OT sampling and ensures that the quasi-OT approach is able to identify the influential parameters from a complex simulation model with high accuracy [24].

To pursue the goal of fixing non-important factors, there is a need to classify the model input

variables. Vanrolleghem et al. [25] proposed a terminology for classification of variables as important/non-important and influential/non-influential using the EE method. A cut-off threshold is determined by the analyst allowing the distinguishing between three different types of variables with respect to the absolute mean (μ^*) and the standard deviation (σ) of the sensitivity measure. In Fig. 10, the line corresponding to $\mu_i^* = 2SEM_i$, where $SEMi$ represents the standard error of the mean, is used for establishing the type of effect of variables [7]. The variable $SEMi$ is equal to $\sigma_i r^{-1/2}$, where r is the number of repetitions. Variables which lie outside the wedge formed by the line corresponding to the established CT_{Morris} and the line $\mu_i^* = 2SEM_i$ have a linear effect on the model outputs. Conversely, the variables which lie inside this area, have a non-linear effect.

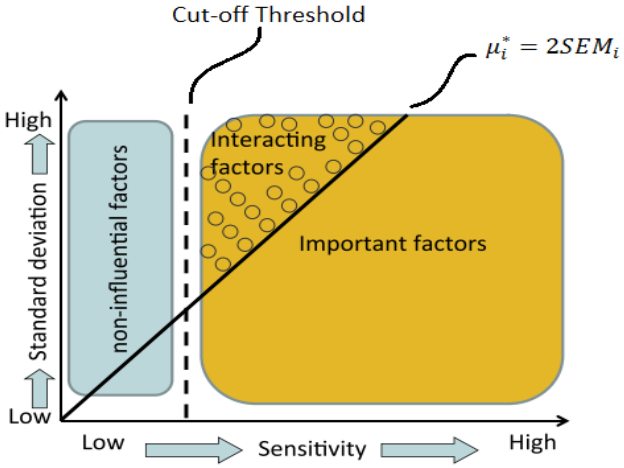

Figure 10. Differentiation of variables in Morris Screening Method [25].

In order to classify the model variables, the cut-off threshold for the Morris-screening (CT_{Morris}) method has to be defined. Thus, the important factors are those that have $\mu_i^* > CT_{Morris}$, the interacting factors have $\mu_i^* > CT_{Morris}$ and $\sigma_i > \mu_i^*\sqrt{r}/2$ while the non-influential factors have $\mu_i^* < CT_{Morris}$.

4. Results and discussions

Table 7 shows the base geometrical parameters and the lower and upper boundaries for sensitivity analysis.

Table 7. Ranges for each geometrical parameter.

Parameter	Base dimensions	Upper dimensions	Lower dimensions
DESL	50%	55%	45%
L1E1	3.37 mm	4.37 mm	2.97 mm
L1E2	11.76 mm	12.76 mm	11.36 mm
L2E1	2.89 mm	3.89 mm	2.49 mm
L2E2	8.82 mm	9.82 mm	8.42 mm
L3E1	2.40 mm	3.40 mm	2.00 mm
L3E2	5.87 mm	6.87 mm	5.47 mm
L4E1	1.92 mm	2.92 mm	1.52 mm
L4E2	2.92 mm	3.92 mm	2.52 mm

Initially it was proposed an approach to discover the impact of each variable on Total-to-Total Isentropic Efficiency. For this, a sampling with nine parameters and ten trajectories was created by

using an implemented model according to Campolongo [8], thereafter this sampling was submitted to ANSYS CFX Solution and the results was analyzed by methodology created by Morris and improved by Campolongo. The results obtained may be encountered in Fig. 11.

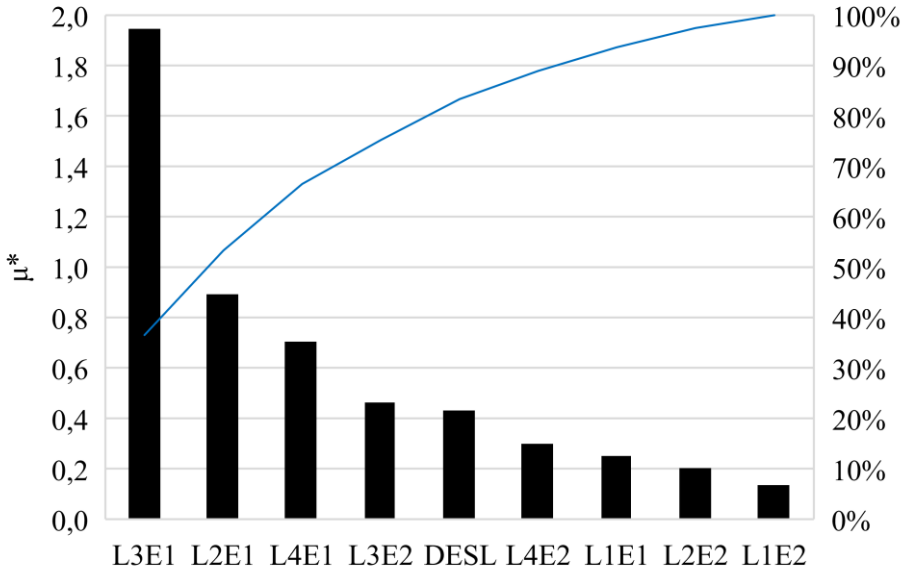

Figure 11. Ranking of input variables main effects (Morris screening method).

By these results, it can be concluded that the third layer is the most influent on efficiency because both thicknesses (inlet and outlet) are among the five most influent while the first layer (hub) is the less influent. It's also possible note that the leading-edge parameters are more significant than those at the trailing edge. In addition, the distance between main blade and splitter appears as the fifth most important parameter. But to decide which one is really influent or negligible the analysis should be subjected to Vanrolleghem terminology that classifies the variables. The results obtained by this approach can be seen in Fig. 12.

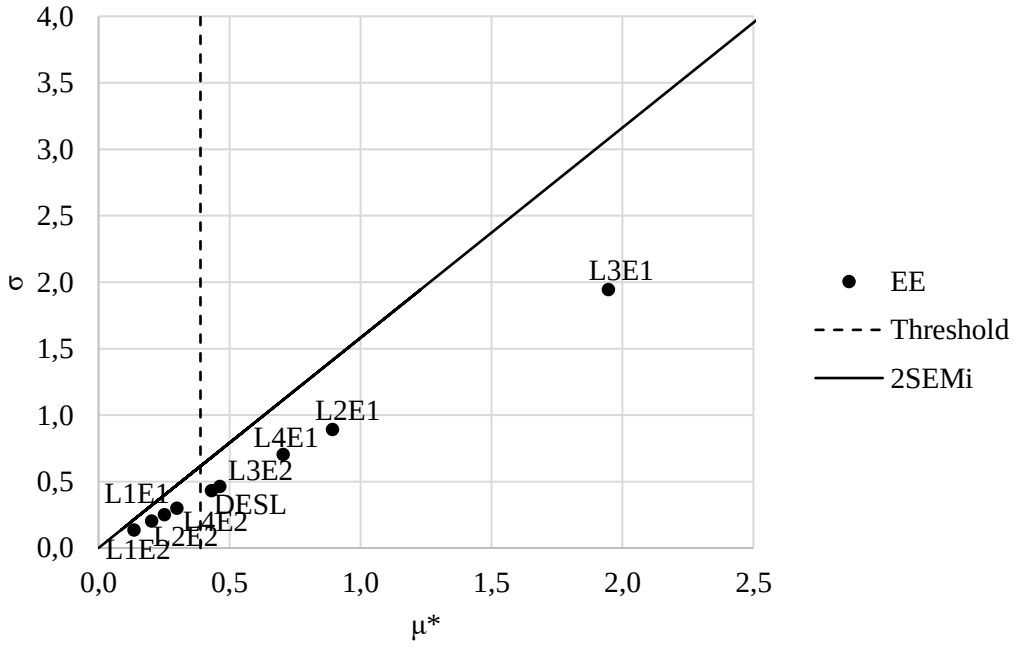

Figure 12. Classification of influential/non-influential parameters.

From there, it is possible to conclude that there are five influent parameters by main effects and

all interaction effects are negligible. They are: both thickness of third layer, leading edge thickness of second and fourth layer and distance between blade and splitter. The threshold was stipulated to ensure that more than 80% of the output variance remains in the model.

To explain this ranking of variables, it was realized a post-processing analysis in ANSYS CFX-Post and two main phenomena were identified as loss sources: a shock wave due to high Mach number on leading edge and a large recirculation present between main blades and splitters that appears at about fifty percent of streamwise and continues until outlet.

Therefore, the rank of variables represents how each parameter deals with such losses. In the case of thicknesses, those that are in medium layers (L3E1, L3E2 and L2E1), when modified, have larger geometric changes than those at the extremities (L4E2, L1E1 and L1E2). Hence, they are the most influent because these changes provide more variations in loss sources. More specifically, leading-edge thicknesses provide bigger changes in shock wave while those at the trailing edge provides in recirculation. The variations observed on efficiency due to recirculation are smaller than those observed due to shock waves what explains the leading edge to be more important.

The fact of leading-edge thickness at third layer be the most influent is a mix of these effects and the Fig. 13 shows that it stands out because it is the region most permeated by shock wave while the second layer is further away and the fourth layer doesn't represent greater changes in geometry.

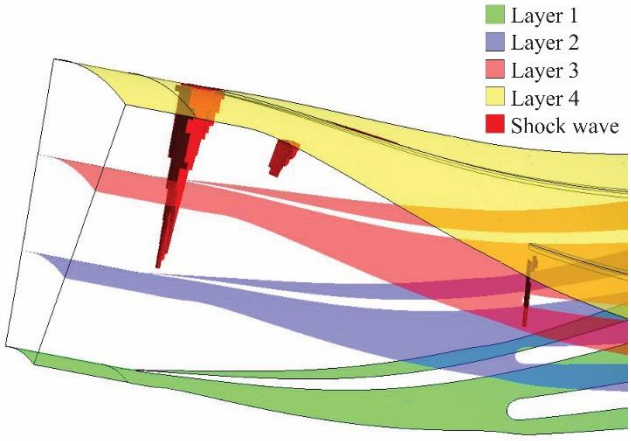

Figure 13. Inlet shock wave

For the single important parameter of trailing edge thicknesses, it is easy to explain because the region with greater eddy viscosity and the center of recirculation focuses exactly on third layer as shown in Fig. 14 and it is clear that a change in this thickness represents a greater change in recirculation region.

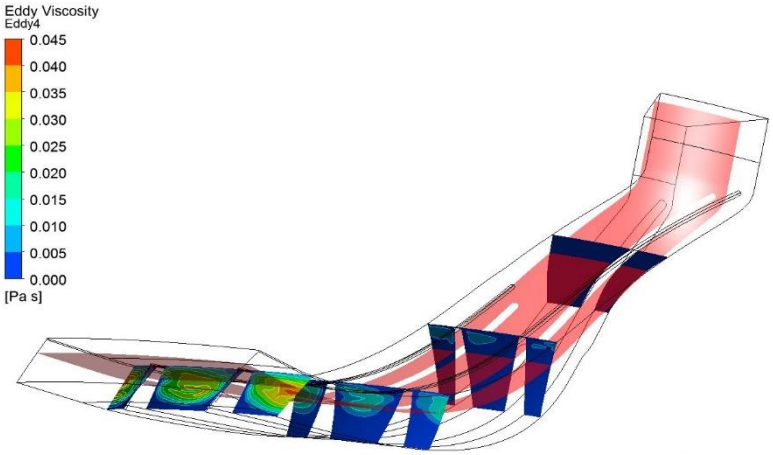

Figure 14. Eddy viscosity through the domain

Finally, for distance between blade and splitter, there is no change in shock wave observed on

leading edge but there is a subtle change in the recirculation shows by Fig. 15 that explain its importance.

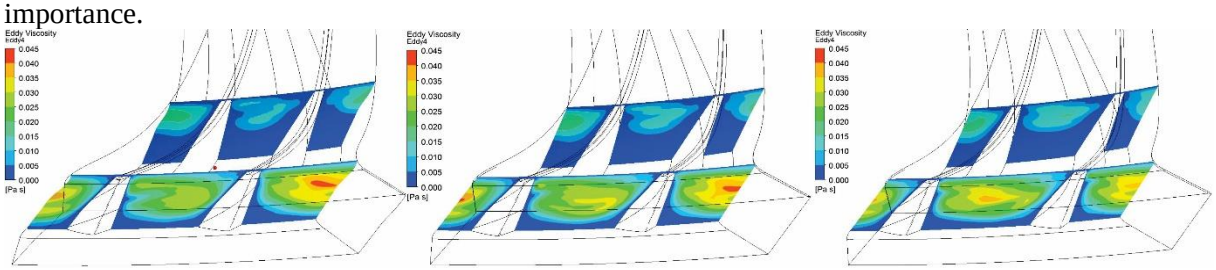

(a) (b) (c)

Figure 15. Eddy viscosity for changes on distance between blade and splitter – (a) 45%, (b) 50% and (c) 55%

5. Conclusions

A Sensitivity Analyze of the blade geometric input parameters in relation to total-to-total isentropic efficiency of a centrifugal compressor called NASA CC3 using Elementary Effects method is presented. The analyze was conducted in a three-dimensional numerical simulation using ANSYS CFX and the discretization was based on parameters implemented on ANSYS Blade Editor. In this software was generated a geometry with four layers in spanwise and two parameters in streamwise that was changing randomly in a sampling strategy proposed by Campolongo.

The work found that the shock waves encountered in leading-edge are a bigger source of losses therefore the thicknesses that are in this region present more influence than others. Furthermore, as the shock waves are encountered in span from 0.33% to 1.00% increasingly it is suggested that the parameters are ranked in this order. But, the medium spanwise thicknesses (L2E1 and L3E1) represent a greater change in geometry, therefore they are more influent than others.

The hub thicknesses can be treated as negligible as seen in the analyze due to this region has low velocities when compared with the remainder domain and presents low changes in the geometry.

The only important parameter at trailing-edge is a thickness at 0.67% of span and it is explained by the recirculation that have its center and the more intensity region exactly on this span.

Finally, the other main parameter is the distance between blade and splitter that proved an influent parameter because its change causes subtle variations on intensity and shape of recirculation.

Although some trends of the influent parameters are identified, exist many other parameters that can be study and proved until more influent than the thicknesses or the meridional distance between blade and splitter. However, this initial study shows that is possible to evaluate the geometric changes in fluid flow behavior and it is important to prepare a model with several parameters to an enhancement.

Acknowledgements

We gratefully acknowledge support of the RCGI – Research Centre for Gas Innovation, hosted by the University of São Paulo (USP) and sponsored by FAPESP – São Paulo Research Foundation (2014/50279-4) and Shell Brasil.

References

[1] L. Blanchette, A. Khadse, M. Mohagheghi, and J. S. Kapat, “Two Types of Analytical Methods for a Centrifugal Compressor Impeller for Supercritical CO2 Power Cycles,” 2016.

[2] M. Casey and C. Robinson, “A new streamline curvature throughflow method for radial turbomachinery,” 2008.

[3] E. Benini, A. Toffolo, and A. Lazzaretto, "Experimental and numerical analyses to enhance the performance of a microturbine diffuser," *Exp. Therm. Fluid Sci.*, vol. 30, no. 5, pp. 427–440, 2006.
[4] M. Marconcini, F. Rubechini, A. Arnone, and S. Ibaraki, "Numerical Investigation of a Transonic Centrifugal Compressor," *J. Turbomach.*, vol. 130, no. 1, p. 011010, 2008.
[5] S. Ibaraki, T. Matsuo, H. Kuma, K. Sumida, and T. Suita, "Aerodynamics of a Transonic Centrifugal Compressor Impeller," 2002, pp. 1–8.
[6] F. Campolongo, A. Saltelli, and J. Cariboni, "From screening to quantitative sensitivity analysis. A unified approach," *Comput. Phys. Commun.*, vol. 182, no. 4, pp. 978–988, 2011.
[7] M. D. Morris, "Factorial Sampling Plans for Preliminary Computational Experiments," *Technometrics*, vol. 33, pp. 161–174, 1991.
[8] F. Campolongo, J. Cariboni, and A. Saltelli, "An effective screening design for sensitivity analysis of large models," *Environ. Model. Softw.*, vol. 22, no. 10, pp. 1509–1518, 2007.
[9] G. J. Skoch, S. P. Prahst, M. P. Wernet, J. R. Wood, and A. J. Strazisar, "Laser Anemometer Measurements of the Flow Field in a 4:1 Pressure Ratio Centrifugal Impeller," Cleveland, Ohio, 1997.
[10] S. Kulkarni, T. A. Beach, and G. J. Skoch, "Computational Study of the CC3 Impeller and Vaneless Diffuser Experiment," pp. 1–12, 2013.
[11] G. J. Hoolbrok and T. F. McKain, "Coordinates for a High Performance 4:1 Pressure Ratio Centrifugal Compressor," Cleveland, Ohio, 1982.
[12] F. R. Menter, "Two-equation eddy-viscosity turbulence models for engineering applications," *AIAA J.*, vol. 32, no. 8, pp. 1598–1605, 1994.
[13] C. Robinson, M. Casey, B. Hutchinson, and R. Steed, "Impeller-Diffuser interection in centrifugal compressors," pp. 1–11, 2012.
[14] P. R. Spalart and M. Shur, "On the Sensitization of Turbulence Models to Rotation and Curvature," *Aerosp. Sci. Technol.*, vol. 1, no. 5, pp. 297–302, 1997.
[15] F. R. Menter, "Review of the shear-stress transport turbulence model experience from an industrial perspective," *Int. J. Comut. Fluid Dyn.*, vol. 23, no. 4, pp. 305–316, 2009.
[16] T. Knopp, T. Alrutz, and D. Schwamborn, "A grid and flow adaptive wall-function method for RANS turbulence modelling," *Journal of Computational Physics*, vol. 220, no. 1. pp. 19–40, 2006.
[17] Y. K. P. Shum and C. S. Tan, "Impeller-Diffuser interaction in Centrifugal Compressor," 2000, pp. 1–12.
[18] "ANSYS CFX-Solver Theory Guide," no. December, 2015.
[19] B. M. Brenes, "Design of supercritical carbon dioxide centrifugal compressors," no. January, pp. 1–151, 2014.
[20] I. B. Celik, U. Ghia, P. J. Roache, C. J. Freitas, H. Coleman, and P. E. Raad, "Procedure for Estimation and Reporting of Uncertainty Due to Discretization in CFD Applications," *J. Fluids Eng.*, vol. 130, no. 7, p. 078001, 2008.
[21] J. P. C. Kleijnen, "Sensitivity Analysis of Simulation Models," *Cent. Discuss. Pap.*, vol. 2009–11, 2009.
[22] N. BILAL, "Implementation of Sobol ' s Method of Global Sensitivity Analysis to a Compressor Simulation Model," *22nd Int. Compress. Eng. Conf. Purdue*, pp. 1–10, 2014.
[23] M. S. and S. T. Andrea Saltelli, Marco Ratto, Terry Andres, Francesca Campolongo, Jessica Cariboni, Debora Gatelli, *Global Sensitivity Analysis. The Primer*. West Sussex, England: John Wiley & Sons Ltd, 2008.
[24] Q. Ge, B. Ciuffo, and M. Menendez, "Combining screening and metamodel-based methods: An efficient sequential approach for the sensitivity analysis of model outputs," *Reliab. Eng. Syst. Saf.*, vol. 134, pp. 334–344, 2015.
[25] P. A. Vanrolleghem, G. Mannina, A. Cosenza, and M. B. Neumann, "Global sensitivity analysis for urban water quality modelling: Terminology, convergence and comparison of different methods," *J. Hydrol.*, vol. 522, pp. 339–352, 2015.